Inhibiting Protein−Protein Interactions: A Model for Antagonist Design

Boris A. Chrunyk, Michele H. Rosner, Yang Cong, Alexander S. McColl, Ivan G. Otterness, and Gaston O. Daumy*

Pfizer Central Research Division, Pfizer Inc., Groton, Connecticut 06340

Received January 18, 2000; Revised Manuscript Received April 11, 2000

ABSTRACT: Protein−protein interactions (PPI) are a ubiquitous mode of transmitting signals in cells and tissues. We are testing a stepwise, generic, structure-driven approach for finding low molecular weight inhibitors of protein−protein interactions. The approach requires development of a high-affinity, single chain antibody directed specifically against the interaction surface of one of the proteins to obtain structural information on the interface. To this end, we developed a single chain antibody (sc1E3) against hIL-1β that exhibited the equivalent affinity of the soluble IL-1 receptor type I (sIL-1R) for hIL-1β and competitively blocked the sIL-1R from binding to the cytokine. The antibody proved to be more specific for hIL-1β than the sIL-1R in that it failed to bind to either murine IL-1β or human/murine IL-1α proteins. Additionally, failure of sc1E3 to bind to several hIL-1β mutant proteins, altered at receptor site B, indicated that the antibody interacted preferentially with this site. This, coupled with other surface plasmon resonance and isothermal titration calorimetry measurements, shows that sc1E3 can achieve comparable affinity of binding hIL-1β as the receptor through interactions at a smaller interface. This stable single chain antibody based heterodimer has simplified the complexity of the IL-1/IL-1R PPI system and will facilitate the design of the low molecular weight inhibitors of this interaction.

Protein−protein interactions (PPI) regulate a large number of important biological functions. Both extracellular and intracellular communication takes advantage of the high degree of specificity afforded by these interactions. Chemotactic factors (C5a, IL-8, etc., and their receptors), cytokines (IL-1,[1] TNF, IL-4, IL-5, IL-6, etc., and their receptors), growth factors (PDGF, TGF etc., and their receptors), integrins, the clotting factors, and complement factor assembly are examples of important PPI systems. These systems provide the organism and the individual cell with specific signals to maintain a well-regulated existence. Despite the importance and prevalence of these interactions, there remains a lack of generic structural approaches for design of specific pharmacologic inhibitors of PPI.

Many PPI provide therapeutically worthwhile targets. However, empirical searches for low molecular weight pharmacological inhibitors (M_r < 400) have routinely failed. These failures have often been attributed to the large surface areas involved between the interacting proteins. At face value, the interface between interacting proteins appears too large (1000−2000 Å^2) to be readily disrupted by small pharmacophores that block only a fraction of this interactive surface. However, Wells and co-workers (*1, 2*) have shown with growth hormone that despite the large area involved in the structural interface, only a few key functional residues can contribute the bulk of the binding energy. Structural information on the energetics of binding between protein antigens and antibodies is also consistent with this view (*3*).

The failure to empirically find low molecular weight compounds that inhibit PPI highlights the need for a rational approach to the design of antagonists. Several ad hoc procedures have shown some success. Sarabu et al. (*4*) have used knowledge of the spatial location of residues R4, K93, and F46 in IL-1β to design a small molecule receptor antagonist with IC_{50} values in the low micromolar range. Some success was obtained by Tien et al. (*5*), who were able to design a small molecule mimic for GCSF. On the other hand, Greene and co-workers (*6, 7*) and others (*8*) have used antibodies in their design process. In particular, Smythe and Itzstein (*8*) designed a biologically active antibody mimic using the crystal structure of a sialidase−antibody complex. This work suggests that antibodies might offer a generic structural approach to the design of small molecule inhibitors. Antibodies are also good blocking agents for PPI, and their interactive surface in most cases comprises the equivalent surface or area of only 6−9 amino acids. This size can be more readily modeled, and there are precedents for downsizing antibodies to smaller molecules (*6, 8*).

We are evaluating a rational, stepwise generic approach to design inhibitors of PPI that entails four phases: (1) mapping the PPI interface of one of the proteins, (2) developing a single chain antibody to the interactive surface, (3) defining the protein−antibody interactive surface, and (4) designing a low molecular weight inhibitor from structural knowledge of the protein−antibody interaction. The underly-

* Correspondence should be addressed to this author at Pfizer Central Research Division, Pfizer Inc., Groton, CT 06340. Phone: (860) 441-3529, Fax: (860) 441-3783, e-mail: gaston_o_daumy@groton.pfizer.com.

[1] Abbreviations: PBS, phosphate buffered saline; TBS, Tris buffered saline; HBS, HEPES buffered saline; mAb, monoclonal antibody; ScFv, single chain antibody; ITC, isothermal titration calorimetry; Ag, antigen; Ab, antibody; sc1E3, single chain antibody 1E3; SPR, surface plasmon resonance; IL-1, interleukin 1; SEC, size-exclusion chromatography; IEF, isoelectric focusing; s-IL-1R, soluble extracellular domain of interleukin 1 receptor type I.

10.1021/bi000096+ CCC: $19.00 © 2000 American Chemical Society
Published on Web 05/26/2000

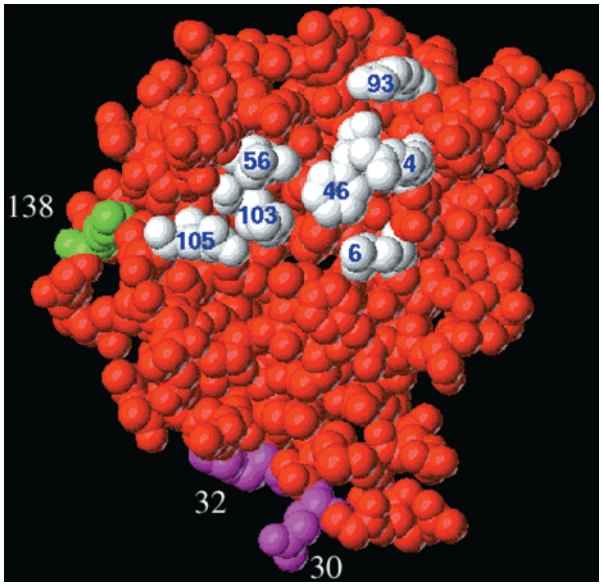

FIGURE 1: Structure of hIL-1β illustrating the location of receptor binding site A (residues 30, 32) and site B (residues 4, 6, 46, 56, 93, 103, 105). The position of K138C mutation is also indicated. Coordinates were taken from Protein Data Bank entry 2I1B (*31*).

ing assumption in this system is that a strong inhibitor interaction involving a few key amino acids can antagonize a high-affinity PPI derived from the cumulative effect of a number of low-affinity interactions.

To test this approach, we have chosen to use the IL-1β/ILR system. The detailed information available on IL-1β and the IL-1 type I receptor (IL1R) suggests that they provide a good model system for studying design of inhibitors of PPI (*4*). Site-specific mutagenesis studies have mapped two separate clusters of amino acids that are absolutely critical to the binding of the IL-1 type I receptor (*9*−*11*). One cluster, designated as site A, is located on the side of the IL-1β β-barrel and comprises residues R11, Q15, H30, and Q32 (Figure 1). This site is common to IL-1α, IL-1β, and the IL-1 receptor antagonist (IL-1ra). The second cluster, site B, is located at the top of the β-barrel and includes residues R4, L6, F46, I56, K93, K103, and E105. Site B binding is a property of IL-1α and -1β, but not of IL-1ra. The recent crystal structure of the IL-1/IL-1R complex has confirmed the importance of these sites derived from mutagenesis studies (*12*). Based on these data, we selected a monoclonal antibody (mAb1E3) that blocked binding between IL-1β and IL-1R (*13*) as the basis for a model system.

We have now downsized the monoclonal antibody to a single chain antibody (sc1E3). The sc1E3 not only blocked the human IL-1β/sIL-R interaction by competing with the receptor for IL-1β binding, but also exhibited a greater specificity for the cytokine than the receptor. More importantly, by using far fewer interactive residues than the receptor, sc1E3 achieved equivalent high-affinity binding, allowing isolation of a stable IL-1β/sc1E3 complex. Such a stable, targeted, single chain antibody based heterodimer has simplified the complexity of the IL-1/IL-1R PPI system and will facilitate the design of the low molecular weight inhibitors of this interaction. The biophysical characterization of 1E3 and its complex formation with IL-1β described here provide proof of concept for the second phase of the rational approach in the development of inhibitors of PPI.

MATERIALS AND METHODS

Preparation of Protein Reagents. Recombinant wild-type human IL-1β (hIL-1β), hIL-1β muteins, and recombinant wild-type murine IL-1α and -1β (mIL-1α and mIL-1β) were prepared as described (*13*−*15*). The soluble recombinant human IL-1 receptor (sIL-1R) and wild-type human IL-1α (hIL-1α) protein preparations were purchased from Genzyme (Cambridge, MA) and Collaborative, Research (Bedford, MA), respectively. The hIL-1β mutein, where lysine 138 was substituted with cysteine (K138C), was used as the parental strain for the other mutants containing alanine substitutions. The K138C mutation had no effect on receptor binding (*13*, *16*, *17*). The rest of the hIL-1β muteins were expected to be deficient in binding to the receptor as they harbored, in addition to the K138C replacement, mutations in one of the receptor binding regions (*9*−*11*). Alanine mutagenesis was used to produce the mutein hIL-1β proteins. Muteins 1 (R4A, L6A), 3 (I56A), 5 (K103A, E105A), and 8 (K93A, K103A, E105A) were purified to near-homogeneity and used to compare receptor binding affinity.

Purification of sc1E3. The sc1E3 Flag-tagged construct was expressed in *E. coli* (Ajith Kamath et al., manuscript in preparation) and purified as follows. The sc1E3 protein was prepared by resuspending cell paste in PBS buffer (1 g wet wt/mL) containing RNase A (0.005 mg/mL), DNase I (0.01 mg/mL), lysozyme (0.24 mg/mL), and $MgCl_2$ (0.0147 M final concentration). After incubation for 30 min at 4 °C, the suspension was subjected to sonic disruption. The enzymes were obtained from Sigma Chemical (St. Louis, MO). The cell suspension was clarified by centrifugation and bound to anti-Flag M2 affinity gel (Eastman Kodak Co., New Haven, CT) in TBS overnight at 4 °C. The gel suspension was packed into a column (25 × 110 mm) and washed with TBS buffer, and the sc1E3 was eluted with 0.1 M glycine buffer (pH 3.5) directly into 1 M Tris buffer, pH 9.0, to achieve a final buffer concentration of 20 mM Tris, pH 7.4. The eluted protein was precipitated by slowly adding solid $(NH_4)_2SO_4$ to 90% saturation. The protein precipitate was recovered by centrifugation, dissolved in PBS, and loaded onto a HiLoad Superdex 75 16/60 column (Amersham Pharmacia Biotech, Piscataway, NJ) in PBS. The fractions containing the monomeric sc1E3 (MW ∼28K) were pooled. The final yield was ∼70 μg of sc1E3 per gram wet weight of cells.

Protein Characterization. The purified proteins were profiled by a series of biochemical tests. SDS−PAGE was performed using 10% Novex NuPAGE gels (Novex, San Diego, CA) in MES running buffer. Gels were stained with Coomassie Brilliant Blue R250. Isoelectric focusing (IEF) was carried out on 3−9 IEF gels with IEF standards (Amersham Pharmacia Biotech). For N-terminal sequencing, samples were run on SDS−PAGE and transferred to Pro-Blott (Applied Biosystems, Foster City, CA) membranes and subjected to sequence analysis. Matrix-assisted laser desorption ionization mass spectrometry (MALDI-MS) was performed on a Voyager MALDI (Perseptive Biosystems, Framingham, MA) calibrated with MALDI protein standards (12−67 kDa) (Hewlett-Packard, Wilmington, DE). Electrospray liquid chromatography mass spectroscopy (ES-LC/MS) analysis was performed on a TSQ700 (Finnigan Corp., San Jose, CA) using a C_4 (0.3 × 300 mm) column (Vydac,

Hesperia, CA) running a gradient from 0 to 100% acetonitrile/0.1% TFA.

Surface Plasmon Resonance (SPR). The K138C mutation introduced in hIL-1β and the alanine muteins derived from it facilitated the preparation of site-specific biotinylated reagents as described previously (*13*). The biotinylated K138C hIL-1β species were immobilized onto streptavidin-derivatized biosensor chips SA5 (BIAcore Inc., Piscataway, NJ) by direct injection. Kinetic analysis of the binding for sIL-1R and sc1E3 to the immobilized forms of K138C and hIL-1β muteins was carried out at low density [i.e., below 100 resonance units (RU)]. Each binding cycle, with sc1E3 in the analyte solution, was performed at a constant flow of 5 μL/min in PBS containing 0.05% Tween 20. The sensor chip was regenerated to the baseline RU after each binding cycle with either 5 or 2.5 mM NaOH, depending on the amount of analyte bound (as gauged by RU). Since dissociation rate constants (k_{off}) are not dependent on analyte concentration, they were determined by flowing saturating concentrations of analyte (e.g., hIL-1R or sc1E3) over the sensor chips to minimize the effect of rebinding. Also, to confirm that rebinding events were not compromising k_{off}, the rates of dissociation were examined in the presence and absence of excess free ligand. In either case, the rates of dissociation were essentially the same. Association rate constants (k_{on}) were determined at different analyte concentrations and averaged. The ratio of k_{off}/k_{on} was used to determine the affinity constant (K_D) of the sIL-1R and sc1E3 for immobilized K138C and hIl-1β muteins. An SPR capture assay was used to measure the interaction between wild-type hIL-1β and the single chain antibody. For the capture binding assay, sc1E3 was first injected onto sensor chips containing immobilized anti-flag antibody (BIA-applications handbook, BIAcore Inc.) followed by an injection of wild-type hIL-1β as the soluble analyte. Anti-flag antibody was chemically coupled to the CM5 sensor chips (BIAcore Inc.) activated by treatment with 1-ethyl-3-[3-(dimethylamino)-propyl]carbodiimide hydrochloride (NHS/EDC). Immobilization of the anti-flag antibody to the chip was done at high density (~3000 RU) and at a constant flow rate (5 μL/min). Multiple injection cycles were performed using a constant concentration of sc1E3 (4.3 μM) followed by different concentrations of wild-type hIL-1β (81 nM to 1.6 μM) as the analyte. To return the baseline back to that of the capturing antibody, both wild-type hIL-1β analyte and the captured sc1E3 ligand were removed with 5 mM NaOH after each cycle. At least 4 cycles of capture binding sets were carried out for the kinetic study. Sensorgrams were analyzed with the BIAevalulation software v2 or v3 by global fitting of the data (BIAcore Inc.). Affinity constants were also measured under equilibrium conditions (K_{eq}) by injection of varying concentrations of sc1E3 (7−450 nM) representing 20−80% ligand (K138C IL-1β) saturation. Once binding equilibrium was achieved, the background RU was subtracted, and the sensorgrams were used to calculate K_D by either linear Scatchard analysis or nonlinear methods. K_D was obtained from the slope of the Scatchard plot to the linear function: $RU_{eq}/C = -1/K_{eq}RU_{eq} + 1/K_{eq}Ru_{max}$, where the RU_{eq} and C represents the RU observed at equilibrium and the concentration of sc1E3 injected, respectively. IC_{50} values from competition studies were determined by plotting log (concentration) vs RU and fitting the experimental points to a sigmoidal equation in Origin (Microcal, North Hampton, MA).

The stoichiometry of the sc1E3/hIL-1β complex by SPR was determined by binding sc1E3 to different immobilized concentrations of IL-1 and comparing the RU bound to the molecular weight ratios: $(RU_{sc1E3}/MW_{sc1E3})/(RU_{hIL\text{-}1\beta}/MW_{hIL\text{-}1\beta})$. For competition experiments with the soluble receptor, sc1E3 was chemically coupled to NHS/EDC-activated CM5 chips, and the binding of a constant concentration (8.8 nM) of wild-type hIL-1β was determined in the presence of different concentrations of soluble IL-1 receptor (0−33 nM).

Size-Exclusion Chromatography. Size-exclusion chromatography (SEC) was carried out in PBS on the SMART system using the Superdex 75 PC 3.2/30 column (Amersham Pharmacia Biotech, Piscataway, NJ). For determination of the apparent Stokes radius (R_s), a BioSelect SEC 125.5 column (300 × 7.8 mm) (BioRad Laboratories, Hercules, CA) was used on a Millenium HPLC system (Waters, Milford, MA). The approximate R_s of the scFv was determined from a standard curve of globular proteins.

Isothermal Titration Calorimetry (ITC). To evaluate binding constants for the sc1E3/hIL-1β complex, sc1E3 was titrated with hIL-1β in PBS (ΔH_{ion} = 1.1 kcal mol^{-1}), HBS (ΔH_{ion} = 5.0 kcal mol^{-1}), and TBS (ΔH_{ion} = 11.3 kcal mol^{-1}), pH 7.0. On average, a total of 15 × 20 μL injections were made. Additionally, hIL-1β was titrated with sc1E3 in PBS. The binding isotherms of ITC are governed by a unitless parameter, c, which is the product of the concentration of binding sites and the affinity constant (*18*, *19*). Binding constants can usually be obtained accurately when the c value is between 5 and 500 (*18*). In our studies, the c value ranged from 37 to 359. Titrations were performed at 20, 25, and 37 °C and in different buffers to determine the change in heat capacity and ionization contributions to the binding, respectively. All titrations were carried out in either a Microcal OMEGA or a VP-ITC calorimeter. Data were analyzed using Microcal ORIGIN for ITC (Microcal, Northhampton, MA).

Analytical Ultracentrifugation. Sedimentation velocity studies were performed on hIL1β, sc1E3, and the antigen−antibody complex at 35, 21, and 2.6 μM, respectively, in PIPES and TBS buffers. Velocity profiles were obtained using UV and interference optics in a Beckman XLI analytical ultracentrifuge (Beckman, Fullerton, CA) using charcoal/Epon cells spinning at 50 000 rpm at 20 °C. The data were fit using the time-derivative method of Stafford (*20*), and $s_{20,w}$ was calculated for each species. Sedimentation equilibrium was done in 20 mM PIPES, 150 mM NaCl, pH 7.5, using isolated complex at concentrations of 4.55, 10.88, and 18.84 μM and speeds of 13 000, 18 000, and 23 000 rpm.

RESULTS

Structural Characteristics of sc1E3. The sc1E3 construct expressed in *E. coli* (Ajith Kamath et al., manuscript in preparation) consisted of the C-terminal end of the light chain variable region of the mAb1E3 joined to the N-terminal end of the heavy chain variable region by a 25 amino acid residue linker (*21*). The sc1E3 protein preparation exhibited a single protein band by SDS−PAGE and by IEF at the predicted M_r of ~28K and pI of 5.5 (Figure 2). LC-ES/MS analysis

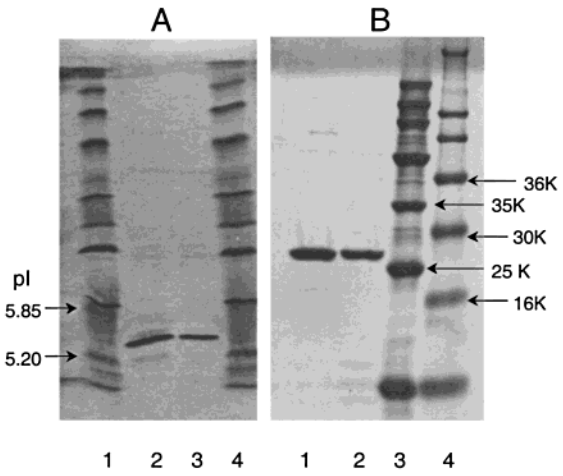

FIGURE 2: IEF and SDS−PAGE of purified sc1E3 preparation. IEF (A) pH 3−9 gels, loaded with 0.1 μg of sc1E3 preparation (lanes 2 and 3) and with IEF protein standards (lanes 1 and 4), were developed by silver staining. SDS−PAGE (12.5%) gels (B), loaded with 4 and 3.4 μg of sc1E3 (lanes 1 and 2) and with molecular weight protein standards (lanes 3 and 4), were developed by Coomassie Blue staining.

yielded a MW of 28 594 (calculated: 28 596), and N-terminal sequence analysis revealed the expected N-terminus of the mAb1E3 light chain.

A Stokes radius of 28.4 Å was calculated for sc1E3 utilizing the retention times on SEC of a subset of standard proteins. The time-derivative sedimentation velocity distribution plots [$g(s)$* plots] for sc1E3 indicated that the individual protein was homogeneous. Sc1E3 exhibited a sedimentation coefficient ($s_{20,w}$) of 2.46 S. A radius of 28.6 Å was calculated for sc1E3 from the sedimentation data, in good agreement with the hydrodynamic radius estimated from SEC.

*Binding Properties of sc1E3 for hIL-1*b. The affinity of sc1E3 for hIL-1β was about 16 nM whether hIL-1β was used as either the soluble or the immobilized ligand or whether hIL-1β was in solution as ITC titrant or SPR analyte (Table 1). A typical SPR sensorgram used to determine K_D values at equilibrium is presented in Figure 3. Figure 4 depicts a typical SPR sensorgram for K_D determination derived from real time on and off rates. As described under Materials and Methods, the rate of dissociation was not compromised by rebinding, as they were the same in the presence or absence of free ligand. The affinity of sc1E3 for K138C hIL-1β was the same as that exhibited by the full-length divalent mAb1E3 parental species for the same ligand (Table 1).

Specificity of sc1E3 Binding to IL-1. The single chain antibody exhibited a similar affinity to sIL-1R for hIL-1β and competed with sIL-1R for IL-1 binding (Figure 5). Also, the recognition profile of sc1E3 paralleled that of the sIL-1R for the site B IL-1β muteins (Table 1). Neither sc1E3 nor sIL-1R recognized mutein 8 while both recognized mutein 3 with affinities comparable to the wild-type hIL-1β (Table 1). Under the conditions tested, sc1E3 failed to recognize mutein 5 and mutein 1 while the affinities of sIL-1R for these muteins were diminished 4- and 9-fold, respectively.

The binding profile of sc1E3 differed from that of IL-1R for other IL-1's. In an SPR competition assay, hIL-1β blocked the binding of both sIL-1R and sc1E3 to immobilized K138C hIL-1β. In addition, both human and murine IL-1α and murine IL-1β competed with sIL-1R for binding to the immobilized K138C IL-1β ligand (Table 2). However, human IL-1α, murine IL-1α, and murine IL-1β failed to block binding of sc1E3 to the ligand even when a large excess of the competitive analyte was used. Thus, under the same competition assay conditions, sc1E3 exclusively recognized hIL-1β (Table 2).

Biochemical Properties of the sc1E3/hIL-1β Complex. Using the ratio method described under Materials and Methods, the SPR data yielded an average stoichiometry of 0.96 mol/mol over four determinations using different concentrations of ligand and analyte (Table 3). ITC titration of sc1E3 with hIL-1β (and hIL-1β with sc1E3) fit well to a single-site model with unitary stoichiometry over nine determinations. A representative ITC binding isotherm is shown in Figure 6. Binding isotherms of hIL-1β with sc1E3 were essentially identical.

A stable complex was formed when hIL-1β and sc1E3 were mixed in approximately 1:1 molar ratios. The complex could be readily isolated by SEC (Figure 7) and could be resolved from both of the reactants. The relative molecular

Table 1: Binding Interactions of sIL-1R and sc1E3 with hIL-1β and hIL-1β Muteins[a]

ligand[b]	titrant/analyte	k_{on} ($\times 10^5$ M^{-1} s^{-1})	k_{off} ($\times 10^{-3}$ s^{-1})	K_D (nM)[c]
K138C hIL-1β	sIL-1R	8.7 (2.2)	3.7 (0.2)	4.3 (0.1)[d]
K138C hIL-1β	sc1E3	7.7 (0.5)	11.0	14.0 (3.8)
sc1E3	hIL-1β	10.0 (1.0)	5.9 (2.8)	6.0 (1.0)[e]
K138C hIL-1β	mAb1E3	NA	NA	28.0 (13.0)[f]
K138C hIL-1β	sc1E3	NA	NA	30.0 (9.0)[f]
sc1E3	hIL-1β	NA	NA	8.7 (0.9)[g]
hIL-1β	sc1E3	NA	NA	6.1 (3.7)[g]
M1 (R4A,L6A)	sIL-1R	2.4 (0.9)	8.7 (0.5)	36.0 (14.0)
M1 (R4A,L6A)	sc1E3			no binding
M5 (K103A,E105A)	sIL-1R	3.5 (0.7)	5.8 (0.3)	16.0 (3.6)
M5 (K103A,E105A)	sc1E3			no binding
M3 (I56A)	sIL-1R	7.1 (<0.1)	4.5 (<0.1)	6.0 (<0.1)
M3 (I56A)	sc1E3	5.8 (0.1)	7.7 (0.3)	13.0 (0.6)
M8 (K93A,K103A,E105A)	sIL-1R			no binding
M8 (K93A,K103A,E105A)	sc1E3			no binding

[a] Numbers in parentheses indicate propagated error through the calculation based on 95% confidence limits on measurables. [b] A letter M followed by a number refers to alanine mutants derived from the K138C parental strain. [c] K_D values were derived from SPR data from the k_{off}/k_{on} ratios. [d] Kinetic values obtained from the literature (*13*). [e] Kinetic value determined by SPR using anti-FLAG capturing assay as described under Materials and Methods. [f] K_D values determined by SPR at equilibrium. [g] K_D values determined by ITC at equilibrium (standard error in parentheses).

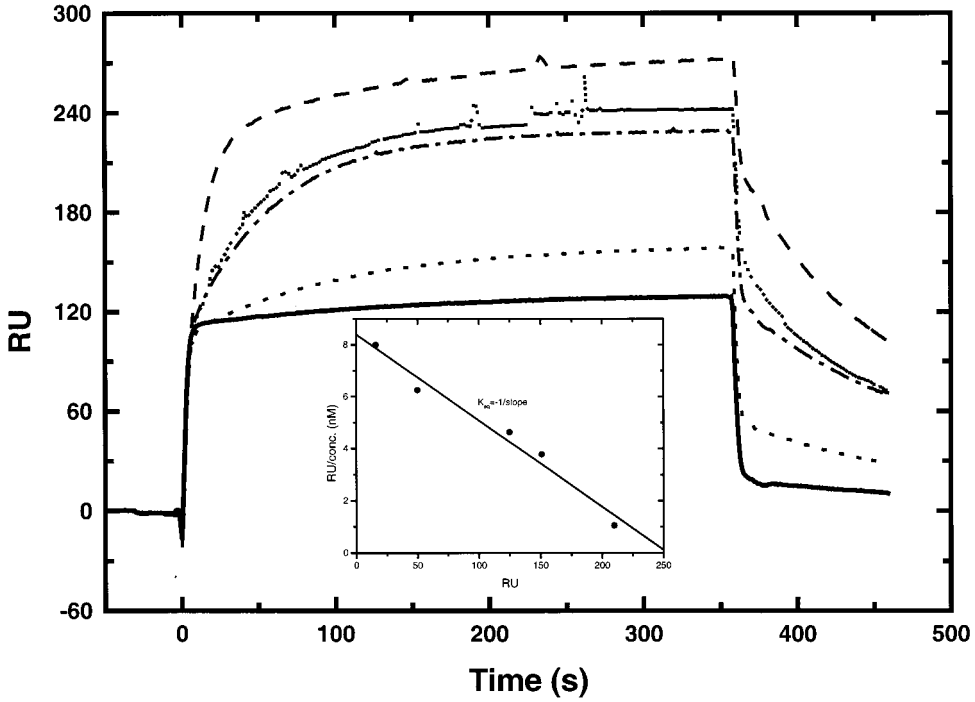

FIGURE 3: Equilibrium dissociation constant determination by SPR. Representative sensorgram of sc1E3 binding to immobilized hIL-1β. The concentrations of sc1E3 used are (shown top to bottom) 200, 40, 27, 8, and 2 nM. The inset depicts Scatchard plot analysis of the data for K_D determination at equilibrium.

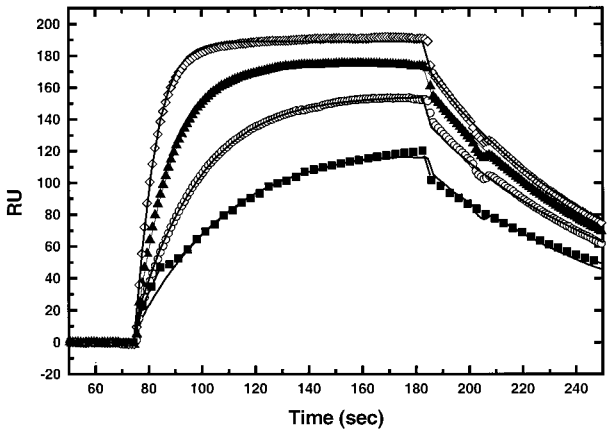

FIGURE 4: Kinetic analyses of sc1E3 binding to K138C hIL-1β by SPR. Representative sensorgram of various concentrations of sc1E3 binding to immobilized IL-1β was used for the determination of k_{off} and k_{on} values (◇, 162 nM; ▲, 85.6 nM; ○, 42.8 nM; and ■, 21.4 nM sc1E3).

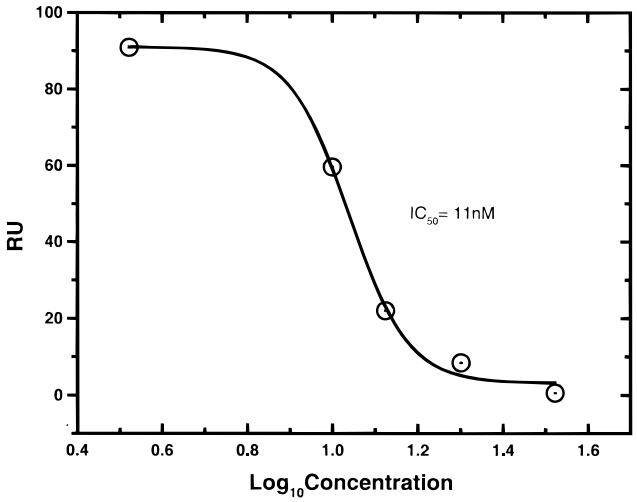

FIGURE 5: Competition between sIL-1R and sc1E3 for hIL-1β binding. The single chain antibody was chemically immobilized onto a sensor chip (590 RU) by amine coupling, and a constant concentration of hIL-1β (8.8 nM) was injected as the analyte. Each injection contained the concentrations of sIL-1R shown in the figure ranging from 0 to 33 nM. The IC_{50} calculated by a sigmoidal fit of the data for sIL-1R was 11 nM.

weight of this complex estimated from SEC was ~43K, and its apparent molecular weight estimated from sedimentation equilibrium was 43.6K (expected 46K). Figure 7 also shows that the complex was not covalently associated through disulfide cross-linking, as it dissociated into its two protein components when subjected to nonreducing SDS−PAGE. In addition, the complex was stable to electrophoresis in native gels (Judith A. Kelly, personal communication). The titrated complex sedimented as a single species based on deconvolution of Gaussians with a sedimentation coefficient of 3.25 S (Figure 8). vanHolde−Weischet analysis (*22*) of this sedimentation data using UltraScan (UTHSCSA, B. Demeler, 1998, 1999) did detect populations of the excess hIL-1β and some of the sc1E3 used in the calorimetric experiment (data not shown). Table 4 lists the thermodynamic parameters obtained from the titrations of the Ag−Ab complex in the three buffer systems and temperatures used in this study. The data indicate that the reaction was enthalpically driven and that the free energy of binding was essentially constant owing to entropy−enthalpy compensation.

DISCUSSION

The objective of this study was to develop a simplified system to enable the rational design of inhibitors of PPI. We chose the IL-1β/IL-1R system because it was very well characterized. It might be thought that because the IL-1β/IL-1R crystal structure has been solved (*12*), that this

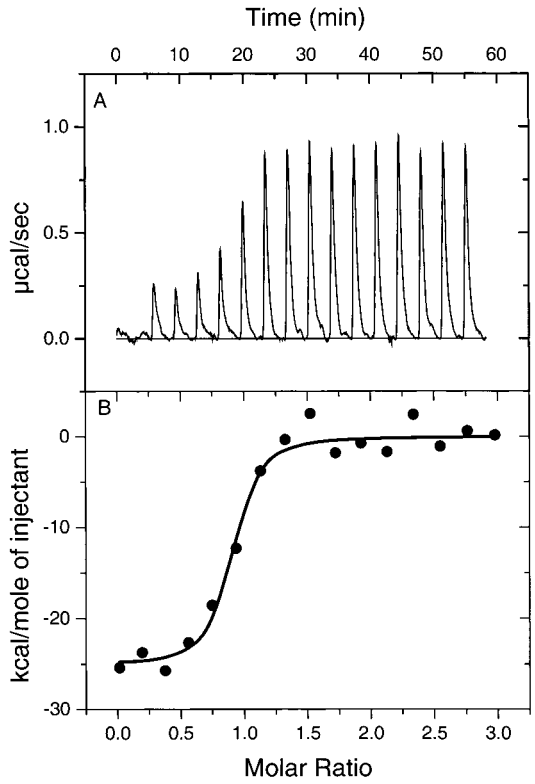

FIGURE 6: ITC binding of hIL1β to sc1E3. (A) Raw thermogram generated by titrating sc1E3 with hIL-1β. The experiment consisted of 15, 20 μL injections of hIL-1β (46.2 μM) into sc1E3 (2.86 μM) in PBS at 37 °C. (B) Binding isotherm generated from integrated data and fitting results using a single site model (Table 4).

information would provide a suitable foundation for designing antagonists. Unfortunately, PPI are distributed over a large surface area comprising many smaller local interactions. A small molecule antagonist can only act at a single site covering a small surface area. This means that blocking of PPI must be based on a very localized high-affinity interaction. Thus, modeling a small molecule inhibitor requires a different approach.

Single chain antibodies can provide a high-affinity interaction with a protein based on binding to a limited number of

Table 2: Comparison of sIL-1R and sc1E3 Binding Specificity for IL-1 Species[a]

analyte	competing analyte	IC_{50} (nM)[c]
sIL-1R[b]	hIL-1β	39 (8)
sc1E3	hIL-1β	4 (0.3)
sIL-1R	hIL-1α	65 (1)
sc1E3	hIL-1α	no competition[d]
sIL-1R[b]	mL-1β	352 (9)
sc1E3	mL-1β	no competition[d]
sIL-1R[b]	mIL-1α	191 (8)
sc1E3	mIL-1α	no competition[d]

[a] K138C IL-1β was used as the ligand and either sIL-1R or sc1E3 as the analyte. To determine the IC_{50}, different IL-1 forms were used as the competing analyte. [b] IC_{50} values for these analytes represent average of independent determinations. [c] Numbers in parentheses indicate propagated error through the calculation based on 95% confidence limits on measurables. [d] No competition was observed when 6, 1000, and 400 times molar excess of hIL-1α, mIL-1β, or mIL-1α, was used, respectively, as the competing analyte.

Table 3: Stoichiometry Determination of sc1E3/hIL-1β Complex Formation by SPR[a]

expt	hIL-1β RU[c] (MW[b] 17.3K)	sc1E3 RU[c] (MW[b] 28.6K)	stoichiometry[d]
1	31.7	53.2	1.02
2	28.8	40.4	0.85
3	115.4	180.7	0.95
4	181.6	312.5	1.04
			av: 0.96

[a] K138C hIL-1β was immobilized at different concentrations for each experiment, and the amount bound of sc1E3 was determined. [b] MW refers to the molecular weights of each individual protein. [c] Resonance units (RU) indicate the amount of immobilized ligand (hIL-1β) and soluble analyte (sc1E3) bound. [d] Stoichiometry represents the ratio of RU/MW ratios: $(RU_{sc1E3}/MW_{sc1E3})/(RU_{hIL\text{-}1\beta}/MW_{hIL\text{-}1\beta})$.

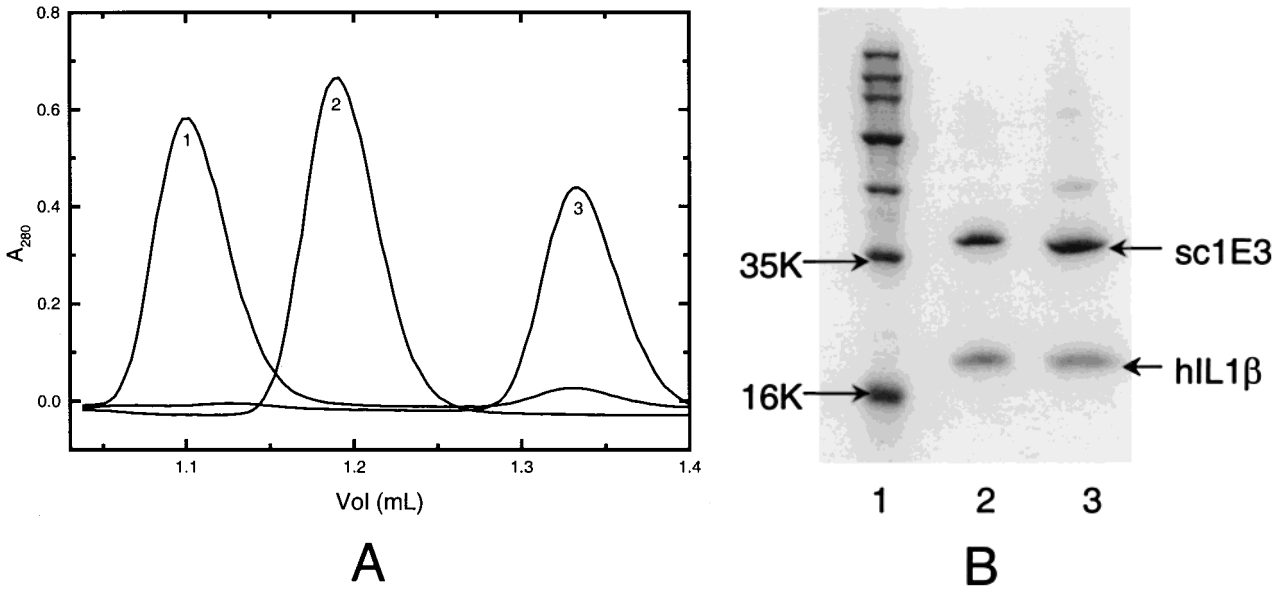

FIGURE 7: Characterization of the sc1E3/hIL-1β complex by SEC and SDS−PAGE. (A) sc1E3 (peak 2), hIL-1β (peak 3), and a ~1:1 molar ratio mixture of each protein (peak 1) were subjected to SEC. The relative molecular weights observed (~26K, ~32K, and ~43K, respectively) were similar to the expected values derived from the sequence (26.K, 17.4K, and 46K, respectively). (B) The sc1E3/hIL-1β complex, isolated from SEC, when subjected to SDS−PAGE, resolved into its two protein components of expected molecular weights in the presence (lane 2) or absence of reducing agents (lane 3). MW standards were loaded in lane 1.

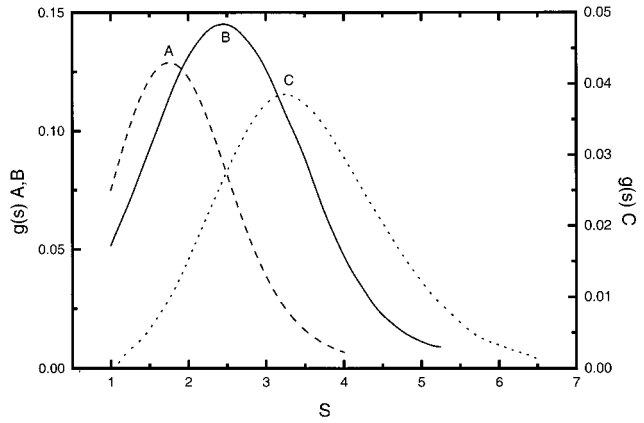

FIGURE 8: Analysis of sc1E3/hIL1β complex formation by sedimentation velocity. Data shown are sedimentation coefficient distributions calculated using the time-derivative method. Samples were run at 60 000 rpm in PIPES buffer, pH 7.2. (A) 21 μM hIL-1β, $s_{20,w}$ = 1.93 S; (B) 35 μM sc1E3, $s_{20,w}$ = 2.46 S; (C) 2.6 μM sc1E3:/hIL-1β complex, $s_{20,w}$ = 3.25 S.

highly localized amino acids. Thus, we conclude that sc1E3/IL-1β provides a better model than IL-1β/IL-1R on which to base design of inhibitors of PPI.

The high-affinity interaction of sc1E3 with hIL-1β was comparable to that achieved with sIL-1R. Muteins of hIL-1β in receptor binding site B (*11*) exhibited decreased affinity for the receptor, yet nearly all failed to bind to sc1E3. Also, while hIL-1α, murine IL-1α, and murine IL-1β competed with hIL-1β for binding to the sIL-1R, they were not able to compete with hIL-1β for binding to sc1E3. Taken together with the competition data, our measurements are consistent with the interpretation that sc1E3 binds the IL-1β molecule at site B and uses fewer, stronger, more local interactions than does sIL-1R.

The comparative SPR data show that sc1E3 utilized a much smaller total binding surface when interacting with human IL-1β than sIL-1R. The bidentate binding of sIL-1R to IL-1α and -1β probably explains why the IL-1α proteins and IL-1β muteins show reduced affinity rather than the total loss of binding affinity as observed for sc1E3. Based on sequence alignments, IL-1α and -1β show only ~20−25% sequence identity with little similarity in the residues involved in site B. Thus, a site B specific single chain antibody might be expected to bind weakly or not at all to IL-1α site B. Though there is high similarity between the murine and human IL-1β sequences (>80%), the flanking residues in strand 1 and in the loop between strands 7 and 8 differ considerably. The inability of sc1E3 to recognize murine IL-1β suggests that some of the binding determinants for sc1E3 may be located in these flanking residues. Interestingly, the I56A protein, which has been identified in the literature as a critical residue for receptor binding (*9, 11*), exhibited wild-type binding to both sc1E3 and receptor. The presence of this I56A mutation was confirmed by DNA sequencing of the clone and by ES-LC/MS of the isolated protein.

A closer examination of the thermodynamics of the system indicates that the binding free energy was relatively constant with temperature, illustrating enthalpy−entropy compensation in the interaction (*23*−*25*). The temperature dependence of the entropy and the fact that the entropy was negative above 0 °C suggested that the interaction is probably driven by hydrogen bond formation and/or van der Waals interactions rather than by hydrophobic interactions (*26, 27*). Selection of buffers with varying ionization enthalpies provides a means to determine proton linkage in the system (*26, 27*). Using the relationship described by Sturtevant (*28*), it was estimated that 0.15 ± 0.07 proton was taken up upon complex formation at 25 °C and ~0.17 ± 0.10 at 37 °C. These low values suggested that the ionization of side chains was not significant to this interaction. The binding enthalpies for the calorimetry data were corrected for this small contribution to the overall enthalpy and are listed in Table 4.

The surface area buried in the interaction and the nature of the surface involved can also be estimated utilizing calorimetric data. The empirical relationships of Murphy and Freire (*23, 29*) were used to calculate the changes in polar (ΔASA_p) and nonpolar (ΔASA_{np}) surface area from the enthalpy and heat capacity data. The heat capacity for the

Table 4: Thermodynamic Parameters Obtained for the Association of hIL-1β with sc1E3

ligand	buffer	temp (°C)	K_a (×1e-7)	ΔH_{rxn}[a] (kcal mol^{-1})	ΔH_b[b] (kcal mol^{-1})	$\Delta G_b°$[c] (kcal mol^{-1})	$\Delta S_b°$[d] (cal mol^{-1})
IL-1β	PBS	25	11.50	−15.0	−15.2	−11.0	−14.2
			(1.17)[e]	(0.1)	(0.1)	(0.1)	(0.3)
IL-1β	PBS	37	4.72	−22.1	−22.2	−11.0	−36.6
			(0.78)	(0.4)	(0.4)	(0.1)	(1.3)
1E3	PBS	25	16.30	−15.6	−15.8	−11.2	−15.3
			(9.90)	(0.3)	(0.3)	(0.3)	(1.6)
1E3	PBS	37	3.86	−16.3	−16.4	−10.8	−18.3
			(0.24)	(0.1)	(0.1)	(0.1)	(0.2)
IL-1β	HBS	25	6.07	−14.5	−15.3	−10.6	−15.6
			(0.19)	(0.2)	(0.2)	(0.1)	(0.8)
IL-1β	HBS	37	4.09	−17.6	−18.3	−10.8	−24.3
			(0.38)	(0.1)	(0.1)	(0.1)	(0.4)
IL-1β	TBS	20	8.39	−13.0	−14.6	−10.6	−13.7
			(3.00)	(0.2)	(0.2)	(0.2)	(2.9)
IL-1β	TBS	25	12.5	−13.8	−15.4	−11.0	−14.8
			(1.14)	(0.1)	(0.1)	(0.1)	(0.3)
IL-1β	TBS	37	5.25	−17.3	−19.0	−10.9	−26.0
			(1.20)	(0.2)	(0.2)	(0.1)	(0.8)

[a] Observed binding enthalpy from calorimetric titration. [b] Binding enthalpy corrected for buffer effects as described in the text. [c] Free energy based on the relationship: $\Delta G° = -RT \ln K_a$. [d] Entropy calculated from the relationship: $\Delta G° = \Delta H° - T\Delta S°$. [e] Values in parentheses reflect error in measurement (K_a) or propagated error in calculation of the parameter.

system was derived from a linear fit of the binding enthalpies for the 20, 25, and 37 °C data in the three buffers. The ΔC_p obtained from the slope of this line was -283 ± 83 cal mol^{-1} K^{-1}. From the data listed in Table 4, the polar accessible surface change at 25 °C was calculated to be 1001 Å^2, while the nonpolar surface was ~1200 Å^2, yielding a total surface involved in the interface of ~2200 Å^2. This value was consistent with most reported Ag−Ab interactions (1600−1900 Å^2) (*24*, *25*, *30*). By comparison, the change in accessible surface area for IL-1β at site B alone, as determined from the crystal structure, was ~1000 Å^2 distributed over 21 residues (*12*). This translates to an almost identical surface occluded (2000 Å^2) in the IL-1R/IL-1 and sc1E3/IL-1 interactions at this site B. To determine how well the nature of the interactions is conserved, a 1.4 Å radius probe molecule was used to calculate the total surface area of the residues involved in IL-1β site B. A total of 2800 Å^2 was determined from this analysis, in which 54% of the surface was found to be polar. Thus, only a fraction of this total surface is occluded in complexation with either the antibody or the receptor at this one site. Similarly, the calculated polar/nonpolar contributions appear to be nearly equally split. Overall, the data suggest that at site B, not only is the total surface area buried comparable, but also the nature of the interactions is reasonably well conserved. However, to achieve high-affinity interaction, the receptor must also bind to hIL-1β at site A and the crystal structure reveals an equivalent of 1087 Å^2 of surface on hIL-1β occluded (~2000 Å^2 total). Therefore, sc1E3 requires only half the total surface area upon binding to IL-1 to achieve the same high-affinity interaction as the receptor.

sc1E3/IL-1β forms a stable complex with the expected 1:1 stoichiometry. This has facilitated complex isolation, and crystals of the complex have been obtained for structural determination (Judith A. Kelly, personal communication). Detailed inhibitor design work will follow the structural specifications derived from the crystal. At this stage, the physical size of sc1E3 makes a significant steric contribution to its ability to inhibit the PPI of IL-1β with its receptor. Downsizing the scFv means in essence decreasing the steric component while maintaining the binding interaction. Decreasing the interaction of IL-1R with IL-1β with a site B specific antagonist will presumably raise the concentration of IL-1β required to cause signal transduction and thereby decrease its pathological effect. We note that we have taken only the first step in antagonist design—establishing a well-characterized model system with which to work.

ACKNOWLEDGMENT

We thank Tom Hynes and Rob Heckel for the construction of the IL-1β muteins, Peter Mezes and Kim Johnson for the construction of sc1E3, and James Blake for the surface area calculations. We also thank Justin Stroh and Tony Lanzetti for their help with mass spectrometry and N-terminal sequencing of some of the reagents used in this study, and Preston Hensley and Judith A. Kelly for their critical review of the manuscript.

REFERENCES

1. Wells, J. A. (1995) *Bio/Technology 13*, 647−652.
2. Wells, J. A. (1996) *Proc. Natl. Acad. Sci. U.S.A. 93*, 1−6.
3. Davies, D., and Cohen, G. (1996) *Proc. Natl. Acad. Sci. U.S.A. 93*, 7−12.
4. Sarabu, R., Cooper, J. P., Cook, C. M., Gillespie, P., Perrotta, A. V., and Olson, G. L. (1998) *Drug Des. Discovery 15*, 191−198.
5. Tian, S.-S., Lamb, P., King, A. G., Miller, S. G., Kessler, L., Luengo, J. I., Averill, L., Johnson, R. K., Gleason, J. G., Pelus, L. M., Dillon, S. B., and Rosen, J. (1998) *Science 281*, 257−259.
6. Saragovi, H. U., Fitzpatrick, D., Raktabutr, A., Nakanishi, H., Kahn, M., and Greene, M. I. (1991) *Science 253*, 792−795.
7. Saragovi, H. U., Greene, M. I., Chrusciel, R. A., and Kahn, M. (1992) *Bio/Technology 10*, 773−778.
8. Smythe, M. L., and von Itzstein, M. (1994) *J. Am. Chem. Soc. 116*, 2725−2733.
9. Evans, R. J., Bray, J., Childs, J. D., Vigers, G. P. A., Brandhuber, B. J., Skalicky, J. J., Thompson, R. C., and Eisenberg, S. P. (1995) *J. Biol. Chem. 270*, 11477−11483.
10. Grutter, M. G., van Oostrum, J., Priestle, J. P., Edelmann, E., Joss, U., Feige, U., Vosbeck, K., and Schmitz, A. (1994) *Protein Eng. 7*, 663−671.
11. Labriola-Tompkins, E., Chandran, C., Kaffka, K. L., Biondi, D., Graves, B. J., Hatada, M., Madison, V. S., Karas, J., Kilian, P. L., and Ju, G. (1991) *Proc. Natl. Acad. Sci. U.S.A. 88*, 11182−11186.
12. Vigers, G. P. A., Anderson, L. J., Caffes, P., and Brandhuber, B. J. (1997) *Nature 386*, 190−194.
13. Cong, Y., McColl, A. S., Hynes, T. R., Heckel, R. C., Mezes, P. S., Lane, C. L., Lee, S. E., Wasilko, D. J., Geoghegan, K. F., Otterness, I. G., and Daumy, G. O. (1997) in *Techniques in Protein Chemistry VIII* (Marshak, D. R., Ed.) pp 523−529, Academic Press, San Diego.
14. Daumy, G. O., Merenda, J. M., McColl, A. S., Andrews, G. C., Franke, A. E., Geoghegan, K. F., and Otterness, I. G. (1989) *Biochim. Biophys. Acta 998*, 32−42.
15. Daumy, G. O., Wilder, C. L., Merenda, J. M., McColl, A. S., Geoghegan, K. F., and Otterness, I. G. (1991) *FEBS Lett. 278*, 98−102.
16. Wingfield, P., Graber, P., Shaw, A. R., Gronenborn, A. M., Clore, G. M., and MacDonald, H. R. (1989) *Eur. J. Biochem. 179*, 565−571.
17. Chollet, A., Bonnefoy, J.-Y., and Odermatt, N. (1990) *J. Immunol. Methods 127*, 179−185.
18. Wiseman, T., Williston, S., Brandts, J. F., and Lin, L. N. (1989) *Anal. Biochem. 179*, 131−137.
19. Freire, E., Mayorga, O. L., and Straume, M. (1990) *Anal. Chem. 62*, 950A−959A.
20. Stafford, W. F., III. (1992) *Anal. Biochem. 203*, 1−7.
21. Whitlow, M., and Filpula, D. (1991) *Methods: Compan. Methods Enzymol. 2*, 97−105.
22. van Holde, K. E., and Weischet, W. O. (1978) *Biopolymers 17*, 1387−1403.
23. Murphy, K. P., Freire, E., and Paterson, Y. (1995) *Proteins: Struct., Funct., Genet. 21*, 83−90.
24. Hibbits, K. A., Gill, D. S., and Willson, R. C. (1994) *Biochemistry 33*, 3584−3590.
25. Raman, C. S., Allen, M. J., and Nall, B. T. (1995) *Biochemistry 34*, 5831−5838.
26. Sturtevant, J. M. (1977) *Proc. Natl. Acad. Sci. U.S.A. 74*, 2236−2240.
27. Baker, B. M., and Murphy, P. K. (1996) *Biophys. J. 71*, 2049−2055.
28. Beres, L., and Sturtevant, J. M. (1971) *Biochemistry 10*, 2120−2126.
29. Murphy, K. P., and Freire, E. (1995) in *Physical Methods to Characterize Pharmaceutical Proteins* (Herron, J. N., Ed.) pp 219−241, Plenum Press, New York.
30. Keown, M. B., Henry, A. J., Ghirlando, R., Sutton, B. J., and Gould, H. J. (1998) *Biochemistry 37*, 8863−8869.
31. Priestle, J. P., Schar, H. P., and Grutter, M. G. (1989) *Proc. Natl. Acad. Sci. U.S.A. 86*, 9667−9671.

BI000096+